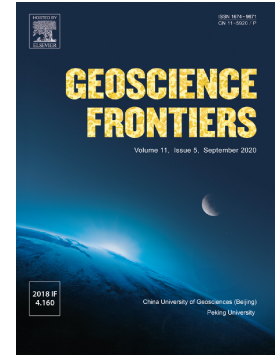# Journal Pre-proof

The influence of fractionation of REE-enriched minerals on the zircon partition coefficients

Shihua Zhong, Sanzhong Li, Reimar Seltmann, Zhiqing Lai, Jie Zhou

Please cite this article as: S. Zhong, S. Li, R. Seltmann, et al., The influence of fractionation of REE-enriched minerals on the zircon partition coefficients, (2020), https://doi.org/10.1016/j.gsf.2020.10.002

This is a PDF file of an article that has undergone enhancements after acceptance, such as the addition of a cover page and metadata, and formatting for readability, but it is not yet the definitive version of record. This version will undergo additional copyediting, typesetting and review before it is published in its final form, but we are providing this version to give early visibility of the article. Please note that, during the production process, errors may be discovered which could affect the content, and all legal disclaimers that apply to the journal pertain.

The influence of fractionation of REE-enriched minerals on the zircon partition coefficients

Shihua Zhong[a,b,*] zhongshihua@ouc.edu.cn, Sanzhong Li[a,b],

Reimar Seltmann[c], Zhiqing Lai[a], Jie Zhou[a,b]

[a]Frontiers Science Center for Deep Ocean Multispheres and Earth System, Key Lab of Submarine Geosciences and Prospecting Techniques, MOE and College of Marine Geosciences, Ocean University of China, Qingdao 266100, China

[b] Laboratory for Marine Mineral Resources, Qingdao National Laboratory for Marine Science and Technology, Qingdao 266237, China

[c] Center for Russian and Central EurAsian Mineral Studies, Department of Earth Sciences, Natural History Museum, London SW7 5BD, UK

[*]**Corresponding author.**

Abstract

Zircon is widely used to simulate melt generation, migration and evolution within the crust and mantle. The achievable performance of melt modeling generally depends on the availability of reliable trace element partition coefficients (D). However, a large range of D_{REE} values for zircon from natural samples and experimental studies has been reported, with values spanning up to 3 orders of magnitude. Unfortunately, a gap of knowledge on this variability is evident. In this study we model the crystallization processes of common REE-bearing minerals from granitic melts and show that the measured zircon D_{REE} would be elevated if there is crystallization of REE-enriched minerals subsequent to zircon. Nevertheless,

compared to zircon D_{REE} values measured from experimental studies, this mechanism appears to have a less significant influence on those from natural granite samples since the quantity of crystallized REE-enriched minerals is very low in natural magmatic systems and/or most of them crystallize prior to zircon. Combined with recently published studies, this work supports that analysis of natural zircon/host groundmass pairs provides more robust D_{REE} values applicable to natural systems than those measured from experimental studies, which can be used to constrain the provenance of detrital zircons.

Keywords: Rayleigh fractionation; Partition coefficient; Fractional crystallization; REE; Zircon

1 Introduction

As a fingerprint of magmatic processes in the Earth's interior, the distributions of trace elements (especially rare earth elements, REEs) in geochemical reservoirs and the corresponding rocks have received considerable attention throughout the last decades (Murali et al., 1983; Blundy and Wood, 1994; Thomas et al., 2002; Shaw, 2006; Tiepolo et al., 2007; Luo and Ayers, 2009; Wagner et al., 2017; Yang, 2019). The behavior of an element between phases involved in a geochemical reaction is generally described by the Nernst partition coefficient "D" (Beattie et al., 1993), which is the ratio of the weight concentration of a trace element in a solid phase divided by its concentration in the equilibrium liquid (Bédard, 2006). Knowledge on D is a prerequisite for quantitatively modelling of magmatic processes. D has been found to be predominantly controlled by magma composition, but for elements with more than one valence, oxygen fugacity may play a significant role (Burnham and Berry, 2012; Trail et al., 2012; Smythe and Brenan, 2015). Temperature, pressure, and crystal chemistry may also control D, but they usually display correlation with melt

composition (e.g., White, 2003).

Zircon ($ZrSiO_4$) is a common accessory mineral in igneous rocks of intermediate to felsic composition. Its ability to incorporate a large number of geochemically important trace elements (e.g., Th-U, Lu-Hf and REEs), as well as the physical-chemical durability and resistance to alteration make it a robust recorder and a unique indicator of many geological processes, such as crustal assimilation, magmatic mixing, crustal recycling as well as evolution of ore-forming magmatic systems (Kemp et al., 2007; Szilas et al., 2013; Van Kranendonk and Kirkland, 2013; Grimes et al., 2015; Roberts and Spencer, 2015; Buret et al., 2016; Lu et al., 2016; Spencer, 2017; Gao and Santosh; 2020; Palin et al., 2020; Xing et al.., 2020). Based on zircon geochemistry, significant interest has also been focused on deciphering likely parental melt provenance of out-of-context grains (e.g., detrital zircons in sedimentary systems) (Grimes et al., 2015). Many of these applications require a better knowledge on zircon D_{REE} (Chapman et al., 2016; Smythe and Brenan, 2016; Burnham and Berry, 2017, 2020; Turner et al., 2020). A large range of D_{REE} values for zircon has been reported, with values spanning up to 3 orders of magnitude, even for zircons that crystallized from a similar melt (Fig. 1). Thus, precise knowledge on this variability is of great significance, e.g., to studies regarding the composition of the earliest Earth crust and to modelling of the growth of the continents (Hanchar and Van Westrenen, 2007).

Theoretically, it is not difficult to obtain the zircon-melt partition coefficients, which can be achieved by measuring the weight concentration of a trace element in zircon crystals and the concentration of the same element in its equilibrium melt. This partition coefficient can be referred to as the "real" partition coefficient. However, in practice, the equilibrium melt composition from which zircon is crystallizing is

generally inaccessible. Even for volcanic rocks, the present groundmass compositions may differ significantly from the melts in equilibrium with the zircon crystals when they grew (Ewart and Griffin, 1994; Hanchar and Van Westrenen, 2007). Thus, the measured partition coefficients in practice are actually "apparent" partition coefficients. Fractional crystallization is a geological process that can probably result in variations of apparent partition coefficients (McIntire, 1963; Jones, 1994). During crystallization of zircon from melts, many REE-bearing (REE-rich) minerals (e.g., apatite, titanite, monazite, feldspar, hornblende) also form. Fractionation of these REE-bearing minerals would not only significantly change the REE contents of melts but also may despoil REEs that should have entered into the zircon crystal lattice, therefore influencing the measured zircon D_{REE} (i.e., the apparent D_{REE}). However, there is little knowledge on the exact effect of fractional crystallization on the measured zircon REE partition coefficients.

In this work, we modelled the crystallization processes of common REE-bearing minerals including zircon, titanite, apatite, plagioclase and amphibole. The aim is to assess the extent to which the measured zircon REE partition coefficients may be influenced by crystallization of these minerals. This is quite different to previous studies which, almost without exception, emphasized the controls of melt composition, temperature and/or oxygen fugacity on zircon D_{REE} (Rubatto and Hermann, 2007; Smythe and Brenan, 2016; Loucks et al., 2018). Using the old Jack Hill zircons as an example, we show that despite the problems the well-constrained D_{REE} from natural zircon/host groundmass pairs can still give a relatively accurate estimate of the parental magmatic melt, which is of great significance for provenance studies of detrital zircons as well.

2 Modelling method

2.1 Starting material

Granitoids are the most abundant rock type in the continental crust, and their generation, segregation, aggregation and emplacement have been a research focus for decades. Although granitic magmas have high viscosity because of their elevated SiO_2 content, fractional crystallization has been commonly reported to be effectively processed during their evolution based on lines of evidence from field investigation, mineral species and their chemical variations, and geochemical compositions (Wu et al., 2017). Most of the REE partition coefficients of zircon published so far are for granitic melts. To facilitate comparison with these results, a starting material of granitic composition is thus an ideal candidate for modelling.

The full REEs of the starting material should be provided to get a better view of compositional variations of melt, zircon and the corresponding partition coefficients during fractional crystallization. The starting melt also should not be characterized by noticeable enrichment or depletion of a certain REE (e.g., Ce and Eu). Considering these constraints, the average composition of intermediate to felsic volcanic rocks from the North China Craton reported by Wang et al. (2006) was used as the starting melt. This granitic melt composition is characterized by a flat chondrite-normalized REE pattern without noticeable Ce and Eu anomalies, which is a suitable starting material.

2.2 Three crystallization scenarios

Three fractional crystallization patterns are considered in this study (Fig. 2): pure zircon crystallization from melt (pattern I), zircon + LateM crystallization (pattern II), and EarlyM + zircon + LateM crystallization (pattern III), where LateM and EarlyM represent minerals that crystallize subsequent and prior to zircon, respectively. In pattern I, the initial melt is assumed to experience pure crystallization of zircon. In

pattern II, it is assumed that only minor zircon grains (which can be neglected quantitatively) form before LateM crystallization. Thus, the remaining melt is still the same as the starting composition until crystallization of the LateM. Pattern III is similar to pattern II except that before zircon crystallization, the initial melt is assumed to have experienced a sufficient crystallization of EarlyM. Titanite, apatite, amphibole and plagioclase, which are all common REE-bearing minerals in magmatic rocks, are considered as EarlyM and LateM in this study.

2.3 Modelling processes

The Rayleigh fractionation model is considered to model the crystallization of REE-bearing minerals, using the following formula (Eq. 1; Rollinson, 1993):

$$C_l = C_l^0 \times F^{(D_R - 1)} \quad (1)$$

where C_l is the concentration of an element in the melt, C_l^0 is the initial element concentration in the melt, F is the fraction of melt remaining, and D_R is the bulk partition coefficient. In this study, since there is no co-crystallizing mineral phase, thus D_R equals to the partition coefficient of the fractionated mineral.

For a certain magmatic system, it is reasonable to assume that the D_R values for REEs are broadly a constant during fractional crystallization process due to the limited variations of temperature, pressure and melt compositions. These values are different from the apparent partition coefficients in the following calculation. In this study, we use mineral-melt partition coefficients listed in Table 1 as real partition coefficients (D_R). These values are used here because that most of D_{REE} are provided within same samples and that their corresponding whole rock compositions are intermediate to felsic, the latter similar to the starting melt composition used by this work.

Zircon composition was calculated using the following formula (Eq. 2):

$C_{\text{Zrn}}^{l} = C_l \times D_R$ (2)

where C_{Zrn}^{l} is the concentration of crystallized zircon which is in equilibrium with

the hypothetical melt of C_l.

The apparent partition coefficients (D) were then calculated using the following

formula (Eq. 3):

$D = \frac{C_{\text{Zrn}}^{l}}{C_l^{F}}$ (3)

where C_l^{F} is the concentration of the final remaining melt. For example, in zircon +

apatite pattern (i.e., pattern B) where apatite experienced 0 to 1 wt.% fractional

crystallization, C_l^{F} is the concentration of the melt that had experienced 1 wt.%

apatite fractional crystallization. For zircon, titanite, apatite crystallization, the

modelling was done for melt fractions from 1 to 0.99, i.e. 0 to 1% mineral

crystallization, in increments of 0.1%. For plagioclase and amphibole crystallization,

this was done for melt fractions from 1–0.6 and 1–0.9, respectively, in increments of

10%. The modelled results of remaining melts and zircon compositions, as well as the

apparent partition coefficients, for the zircon + apatite crystallization pattern are

presented in supplementary material as an example (Suppl. Table S1).

3 Results

Fig. 3 shows the REE variations of the remaining melt and crystallized zircon, as

well as changes of measured partition coefficients under the pure zircon

crystallization scenario (pattern I). Although noticeable variations of the LREE

contents are not observed, it is shown that the HREE contents of the remaining melt

vary significantly with progressing zircon crystallization (Fig. 3A). In turn, the zircon

compositions also change consistently to maintain the equilibrium with the remaining

melt (Fig. 3B). Fig.3C shows the modelled results of zircon REE partition coefficients

when the original melt finally experiences 1 wt.% zircon crystallization. It can be seen that for zircon formed earlier, elevated (and thus wrong) D_{HREE} values are manifested. The earlier the zircon forms, the bigger the errors are. In contrast, the calculated zircon D_{LREE} values do not vary (at least visually) with fractional crystallization.

Fig. 4 shows the modelling results of the remaining melt, zircon and the measured partition coefficients under the second crystallization scenario (pattern II), using apatite as the LateM. In this pattern, the melt composition and the apparent D_{REE} of zircon are strictly controlled by apatite fractional crystallization. Different to pattern I, late apatite crystallization will not only result in overestimation of D_{HREE}, but also of D_{LREE}. Using plagioclase and apatite as EarlyM and LateM, respectively, Fig. 5 models the third crystallization scenario (pattern III). It is shown that the observed D_{REE} values of zircon are totally same to pattern II, indicating that the crystallized REE-bearing minerals prior to zircon show no effect on zircon partition coefficients.

In supplementary material we also modelled crystallization of other REE-bearing minerals (Suppl. Fig. S1–S3). They gave similar results to Figs. 4 and 5 and showed that the measured partition coefficients may be over-estimated if there is significant crystallization of REE-bearing minerals subsequent to zircon.

4 Discussion

4.1 Influence of fractionation on the measured zircon-melt D_{REE}

The new results show that the measured zircon REE partition coefficients may be elevated by 1–2 orders of magnitude if there are accessory minerals that crystallize subsequent to zircon (Figs. 3–5 and Suppl. Figs. S1–S3). Significant crystallization of zircon itself will have a similar effect. This is owed to that in practice we generally use the groundmass surrounding zircon as its parental melt during calculations of

zircon partition coefficients, whereas it may be vastly different from the true compositional environment when zircon is crystallizing. To which degree D_{REE} will be elevated depends on the REE patterns and quantity of minerals that crystallize after zircons. For example, all zircon REE partition coefficients tend to show high values with crystallization of apatite subsequent to zircon, whereas extensive zircon crystallization will only elevate D_{HREE} values. It is noted that for pure zircon crystallization, the errors of the measured HREE partition coefficients depend on its crystallization time: with progressing zircon crystallization, the remaining melt is no longer in equilibrium with crystallized zircon grains, so the earlier the zircon grains form, the bigger the errors of the partition coefficients are. In contrast, minerals that crystalize prior to zircon do not have an influence on the measured zircon D_{REE}. However, they will influence the final trace element patterns of zircons and remaining melts. Therefore, whether the measured zircon D_{REE} is precise would partly depend on the available information on their parental melt crystallization history.

A crystallization scenario that has not been modelled here is that REE-bearing minerals can form simultaneously with zircon, which we think will play a similar role to the scenario of pure zircon crystallization. These minerals crystallizing simultaneously with zircon grains can enhance the changes of the local environment from which zircon grows, the degree depending on both their quantity and compositions. This may explain the oscillatory zoning widely observed within magmatic zircon grains, although variations in zircon growth rate and diffusion-controlled chemical feedback are also possible mechanisms (Halden and Hawthorne, 1993; Fowler et al., 2002; Shaw, 2006). Thus, it is easily deduced that REE-bearing minerals co-crystallizing with zircon can also influence the measured zircon D_{REE} to some degree. As stated by Burnham (2020), sector-specific partition

coefficients of zircon may be necessary to give the most accurate inversions of melt REE concentrations in future.

4.2 Robustness of published zircon-melt D_{REE}: experimental studies vs. natural samples

As mentioned earlier, a number of zircon D_{REE} values (and also other trace element partition coefficients) have been reported so far, which can span up to 3 orders of magnitude for the same element. These partition coefficients can be broadly divided into two groups according to the sources of zircons: experimental studies (synthesized zircons) and natural samples (natural grains). It is not a trivial matter to know which group (or which one) is more credible considering the significant applications of zircon D_{REE} values.

4.2.1 The existing problems

Experimental studies were designed to obtain zircon D_{REE} (and also other trace element partition coefficients) by growing zircon from synthesized trace-element doped melts. But some of them were conducted in extreme temperature and pressure conditions notably different to natural systems (Burnham and Berry, 2012), therefore limiting the application of these REE partition coefficients to natural zircon samples. For experimental studies carried out under the physical-chemical conditions similar to natural magmatic systems, the measured D_{REE} values for synthesized zircons probably still cannot accurately reproduce the fractionation factors of natural systems. The reasons are as follows.

(1) Zircon crystals growing in the laboratory are generally small with size from <1 μm to 20 μm, and thus accurate measurements of trace elements are extremely challenging if the accidental sampling of mineral/melt inclusions occurs (Zhong et al., 2018, 2019). This is because the spot sizes of routine *in situ* analysis equipment are

generally >20 μm; therefore most, if not all, synthesized zircons were not large enough to allow accurate measurements (Ayers et al., 2003; Hanchar and Van Westrenen, 2007). Thus, it is not strange in Fig. 1 that experimental studies normally reported higher D_{LREE} values than natural samples, which are probably derived from a contaminated zircon composition by LREE-enriched mineral/melt inclusions(Rubatto and Hermann, 2007; Zhong et al., 2018).

(2) All the published experiments were designed to facilitate rapid zircon growth during an experimental time frame of days to weeks (contrasting with at least several thousand years in natural magmatic systems) (Hanchar and Van Westrenen, 2007). This resulted in disequilibrium partitioning caused by boundary-layer, which does not likely develop in natural systems since the rate of zircon growth is less than the rate of diffusion in the fluid/melt (Luo and Ayers, 2009). Thus, the measured D_{REE} values might be disequilibrium ones and therefore in error.

(3) The xenotime substitution mechanism ($REE^{3+}+P^{5+}=Zr^{4+}+Si^{4+}$) is normally used to introduce the REE from experimental melts into synthetic zircons (e.g., Burnham and Berry, 2012), which may be different from natural samples (Hoskin and Ireland, 2000). Fig. 6 shows REE (plus Y) and P values of 952 natural zircon grains from GEOROC database. It can be seen that a positive correlation between REE+Y and P, which is expected if the xenotime substitution mechanism exists in these zircon grains, is not clearly manifested. This indicates that for natural zircon grains, the xenotime substitution mechanism is not the only mechanism to incorporate REEs (Perez-Soba et al., 2007; Breiter et al., 2014; De Hoog et al., 2014). A recent study by Burnham and O'Neill (2019) also pointed out that a trace element may substitute into a mineral by more than one substitution mechanism, and that the measured partition coefficients are often the sums of contributions from multiple substitution

mechanisms.

Therefore, considering these problems, the zircon partition coefficients obtained from experimental studies are seemingly less credible than those from natural samples.

4.2.2 Fractional crystallization of REE-enriched minerals

Apart from the above problems, the modelling result in this study also suggests that the D_{REE} values obtained from natural samples seem more plausible. This is because the (fractional) crystallization of REE-enriched minerals in natural samples may not be a predominant process. REE-enriched minerals (including titanite, apatite, zircon and monazite) in natural magmatic rocks normally constitute a low volume percentage. Besides, apatite, titanite, monazite generally occur as mineral inclusions in zircon from magmatic rocks whereas zircon relatively seldom occurs as inclusions in those minerals, indicating that most of them may crystallize before zircon in natural systems. Moreover, Fig. 7 shows that if significant REE-enriched mineral crystallization after zircon (including zircon itself) exists for granitic melts, uncommon REE patterns of zircons and/or groundmass (i.e., the remaining melt) will be observed, which however are not reported in the literature. Thus, all these lines of evidence points to the conclusion that in natural samples the quantity of REE-enriched minerals that crystallize after zircon, if any, should be very low, and that analysis of natural zircon/host groundmass pairs (volcanic rocks) should provide more robust zircon-melt partition coefficients applicable to natural systems (Ewart and Griffin et al., 1994).

Particularly, many studies advocate the measurements of Sano et al. (2002), characterized by lowest D_{LREE} can reproduce the melt compositions (at least for felsic melts) that are more comfortable to available geological evidence (Hanchar and Van

Westrenen, 2007; Luo and Ayers, 2009; Smythe and Brenan, 2016). We agree with this since the low D_{LREE} reported by Sano et al. (2002) is consistent with our recent study which showed that magmatic zircons may be characterized by extremely low LREE contents (Zhong et al., 2019). However, it is noted that not all the natural samples can give credible zircon partition coefficients. Compared to volcanic rocks, the exact melt compositions from which zircons crystalize are hard to access for intrusive rocks, which inhibits their applications in pursuing high-quality measurements of zircon partition coefficients. Alternatively, many studies have used whole-rock composition of intrusive rocks as an equivalent of melt composition during the partition coefficient calculation of zircon, which however is problematic and could incur errors according to our modelled result. Thus, to obtain high-quality zircon partition coefficients, currently volcanic rocks and also perhaps melt inclusions may be the most ideal candidates.

In contrast to natural samples, for experimental studies the degree of crystallization of REE-enriched minerals (especially zircon itself) can be high. To show the possible variations of partition coefficients under this circumstance, in Fig. 7 we show the modelling results for 0–5% pure zircon crystallization (Fig. 7A, B; corresponding to pattern I) and 0–5% apatite crystallization after zircon (Fig. 7C, D; corresponding to pattern II), respectively, although both scenarios may be unrealistic for natural samples. It can be seen that in both scenarios the zircon D_{REE} may be overestimated by more than three orders of magnitude (Fig. 7). The experimental study of Luo and Ayers (2009) may represent such an example. Luo and Ayers (2009) showed that the synthesized zircons from trace-element doped hydrous peralkaline rhyolite melts could make up 5% of the run products (indicating significant zircon crystallization), and that the measured zircon D_{REE} varied within different runs. They

attributed the variations of D_{REE} to that time was required to reach a steady state (Luo and Ayers, 2009). This is possible but cannot fully explain why only partition coefficients for Gd, Lu, Y (and thus HREEs) and U varied with time, whereas those for Pr, Nd and Eu (and thus M- and LREEs) did not show visible variations. According to our study, this variation pattern of D_{REE} can be well explained by significant (fractional) crystallization of zircon (Fig. 7). This is because zircon (fractional) crystallization will only result in noticeable variations of the measured D_{HREE} values, whereas D_{LREE} values are nearly not affected (Fig. 7B). Thus, it is reasonable to deduce that zircon D_{HREE} may be overestimated by those experimental studies.

However, contrary to our prediction, in Fig. 1 one of seven experimental studies gives similar D_{HREE} values to natural samples, whereas all other experimental studies (including two of Luo and Ayers' works) even show much lower D_{HREE} values than natural samples. Nevertheless, this does not necessarily suggest that crystallization of zircon in those experimental studies was not as strong as our prediction, or that the role of fractionation on zircon partition coefficients is amplified by our modelling method; rather, we believe this reflects that zircon partition coefficients are affected not merely by one or two factors but by multiple factors, which have diverse degrees of effect on the measured values. Here, we do not enter into the debate whether the thermodynamic parameters (e.g., temperature, pressure) (Rubatto and Hermann, 2007; Luo and Ayers, 2009) or melt compositions (Hoskin and Schaltegger, 2003; Hanchar and Van Westrenen, 2007) are predominant in accounting for the observed variations; rather, we propose a new explanation without involvement of the above parameters. In almost all these experimental studies, phosphorus was added which was used as the only tool for the charge balance (based on the xenotime substitution mechanism). This

may inhibit a sufficient incorporation of HREE into zircons (and thus results in low D_{HREE}) since in natural systems more than one charge balance mechanism exists (De Hoog et al., 2014).

4.3 Implications for provenance studies of detrital zircon

To use REE partition coefficients for zircon to calculate equilibrium melt compositions is an important application of zircon, especially in the case of detrital zircon for which the source-rock composition is most likely not known (Hanchar and Van Westrenen, 2007). However, the observed large variation of zircon/melt partitioning, as manifested in Fig. 1, shows that recalculation of melt compositions from zircon is quite difficult. Indeed, with so little known about the exact growth environments of zircons, e.g., temperature, pressure, melt composition, as well as charge balance mechanisms within the zircon lattice, it is inevitable that any analogue study will be imperfect to characterize the structure of their parental melts and that different studies may even get contrary results. Nevertheless, by examining the available growth information of zircons (e.g., temperature and pressure are normally known for experimental studies) and the modelling results, we can identify geochemical trends of partition coefficients and attempt to relate these to old, enigmatic samples such as the Jack Hill zircons.

The detrital zircon grains from the Jack Hills, Australia, are the oldest known terrestrial objects and contain the record for the early Earth (Wilde et al., 2001; Roberts and Spencer, 2015). There is a consensus that these Hadean detrital zircon grains are of magmatic origin, but thereafter opinions differ. Some studies advocate I-type granites as source rocks (Burnham and Berry, 2017), whereas others infer basaltic source rocks (Coogan and Hinton, 2006; Dhuime et al., 2015). An impact melt source is also proposed considering the high frequency of meteorite impacts

(Kenny et al., 2016). The most recent study, in contrast, proposed andesites formed in modern subduction settings as their protoliths (Turner et al., 2020). Here, we do not enter into the debate about the causes of the distinct conclusions; rather, using zircon D_{REE}, we reconstruct the REE patterns of the melts from which Jack Hill zircons crystallized, and compare them with the possible protolith types proposed by previous studies. It is shown that the zircon D_{REE} from natural samples indicate a LREE-enriched source rocks, which is different from the experimental database which indicate a slightly HREE-enriched protoliths (Fig. 8). According to above discussions, the LREE-enriched feature constrained by partition coefficients from natural samples is probably a real feature of the parental melt that crystallized Jack Hill zircons, which thus advocates a granitic (crustal) protolith (Luo and Ayers, 2009).

5 Conclusions

These new results show that the fractionation of REE-enriched minerals subsequent to zircon can influence the measured zircon D_{REE} and thus to obtain precise partition coefficients will require a background knowledge on the crystallization history of REE-bearing minerals in rocks. This finding also can be extrapolated to empirical partition coefficient studies of many other minerals (e.g., apatite and titanite), which have a similar role for quantitatively modelling melt generation, migration and evolution within the crust and/or mantle. Nonetheless, both the petrological observations and the modelling results for REE patterns of natural samples suggest that the quantity of crystallized REE-enriched minerals should be very limited and/or many of them formed prior to zircon in natural systems. This, combined with published studies, supports that analysis of natural zircon/host groundmass pairs from volcanic rocks and/or melt inclusions should provide more robust empirical zircon/melt partition coefficients applicable to natural systems than

those measured from experimental studies. Nevertheless, well designed experimental studies are still required and promising to develop a clearer understanding of the natural processes governing zircon–melt REE partitioning.

Acknowledgements

Declaration of interests

☒ The authors declare that they have no known competing financial interests or personal relationships that could have appeared to influence the work reported in this paper.

Supplementary data

Supplementary material

References

Ayers, J.C., DeLaCruz, K., Miller, C., Switzer, O., 2003.Experimental study of zircon

coarsening in quartzite $\pm H_2O$ at 1.0 GPa and 1000 °C, with implications for geochronological studies of high-grade metamorphism. American Mineralogist 88, 365-376.

Beattie, P., Drake, M., Jones, J., Leeman, W., Longhi, J., McKay, G., Nielsen, R., Palme, H., Shaw, D., Takahashi, E., 1993. Terminology for trace-element partitioning. Geochimica et Cosmochimica Acta 57, 1605-1606.

Bédard, J.H., 2006. Trace element partitioning in plagioclase feldspar. Geochimica et Cosmochimica Acta70, 3717-3742.

Blundy, J., Wood, B., 1994.Prediction of crystal-melt partition coefficients from elastic moduli. Nature 372, 452-454.

Breiter, K., Lamarão, C.N., Borges, R.M.K., Dall'Agnol, R., 2014. Chemical characteristics of zircon from A-type granites and comparison to zircon of S-type granites. Lithos 192-195, 208-225.

Buret, Y., von Quadt, A., Heinrich, C., Selby, D., Wälle, M., Peytcheva, I., 2016. From a long-lived upper-crustal magma chamber to rapid porphyry copper emplacement: Reading the geochemistry of zircon crystals at Bajo de la Alumbrera (NW Argentina). Earth and Planetary Science Letters 450, 120-131.

Burnham, A. D., 2020. Key concepts in interpreting the concentrations of the rare earth elements in zircon. Chemical Geology 551, 119765.

Burnham, A.D., Berry, A.J., 2012. An experimental study of trace element partitioning between zircon and melt as a function of oxygen fugacity. Geochimica et Cosmochimica Acta 95, 196-212.

Burnham, A.D., Berry, A.J., 2017. Formation of Hadean granites by melting of igneous crust. Nature Geoscience 10, 457-461.

Burnham, A.D., O'Neill, H.S.C., 2019. Mineral–melt partition coefficients and the problem of multiple substitution mechanisms: insights from the rare earths in forsterite and protoenstatite. Contributions to Mineralogy and Petrology 175, 7.

Cavosie, A.J., Valley, J.W., Wilde, S.A., 2006. Correlated microanalysis of zircon: Trace element, $\delta^{18}O$, and U–Th–Pb isotopic constraints on the igneous origin of complex >3900Ma detrital grains. Geochimica et Cosmochimica Acta 70, 5601-5616.

Chapman, J.B., Gehrels, G.E., Ducea, M.N., Giesler, N., Pullen, A., 2016. A new method for estimating parent rock trace element concentrations from zircon. Chemical Geology 439, 59-70.

Colombini, L.L., Miller, C.F., Gualda, G.A., Wooden, J.L., Miller, J.S., 2011. Sphene and zircon in the Highland Range volcanic sequence (Miocene, southern Nevada, USA): elemental partitioning, phase relations, and influence on evolution of silicic magma. Mineralogy and Petrology 102, 29-50.

Coogan, L.A., Hinton, R.W., 2006. Do the trace element compositions of detrital zircons require Hadean continental crust? Geology 34, 633-636.

De Hoog, J.C.M., Lissenberg, C.J., Brooker, R.A., Hinton, R., Trail, D., Hellebrand, E., 2014. Hydrogen incorporation and charge balance in natural zircon. Geochimica et Cosmochimica Acta 141, 472-486.

Dhuime, B., Wuestefeld, A., Hawkesworth, C.J., 2015. Emergence of modern continental crust about 3 billion years ago. Nature Geoscience 8, 552-555.

Dunn, T., Sen, C., 1994. Mineral/matrix partition coefficients for orthopyroxene, plagioclase, and olivine in basaltic to andesitic systems: A combined analytical and experimental study. Geochimica et Cosmochimica Acta 58, 717-733.

Ewart, A., Griffin, W. L., 1994. Application of proton-microprobe data to trace-element partitioning in volcanic rocks. Chemical Geology 117, 251-284.

Fowler A, Prokoph A, Stern, R.,Dupuis, C., 2002. Organization of oscillatory zoning in zircon: analysis, scaling, geochemistry, and model of a zircon from Kipawa, Quebec, Canada. Geochimica et Cosmochimica Acta 66, 311-328.

Gao, P., Santosh, M., 2020. Mesoarchean accretionary mélange and tectonic erosion in the Archean Dharwar Craton, southern India: Plate tectonics in the early Earth. Gondwana Research 85,291-305.

Grimes, C., Wooden, J., Cheadle, M., John, B., 2015."Fingerprinting" tectono-magmatic provenance using trace elements in igneous zircon. Contributions to Mineralogy and Petrology 170,1-26.

Halden, N.M., Hawthorne, F.C., 1993. The fractal geometry of oscillatory zoning in crystals: Application to zircon. American Mineralogist 78, 1113-1116.

Hanchar, J.M., Van Westrenen, W., 2007, Rare earth element behavior in zircon-melt systems. Elements 3, 37-42.

Hoskin, P., Black, L., 2000. Metamorphic zircon formation by solid-state recrystallization of protolith igneous zircon. Journal of Metamorphic Geology 18, 423-439.

Hoskin, P.W., Schaltegger, U., 2003. The composition of zircon and igneous and metamorphic petrogenesis. Reviews in Mineralogy and Geochemistry 53, 27-62.

Jones, J.H., 1994. Fractional crystallization of iron meteorites: Constant versus changing partition coefficients. Meteoritics 29, 423-426.

Kemp, A., Hawkesworth, C., Foster, G., Paterson, B., Woodhead, J., Hergt, J., Gray, C., Whitehouse, M., 2007. Magmatic and crustal differentiation history of

granitic rocks from Hf-O isotopes in zircon. Science 315, 980-983.

Kenny, G.G., Whitehouse, M.J., Kamber, B.S., 2016. Differentiated impact melt sheets may be a potential source of Hadean detrital zircon. Geology 44, 435-438.

Loucks, R.R., Fiorentini, M.L., Rohrlach, B.D., 2018. Divergent $T–fO_2$ paths during crystallisation of H_2O-rich and H_2O-poor magmas as recorded by Ce and U in zircon, with implications for TitaniQ and TitaniZ geothermometry. Contributions to Mineralogy and Petrology 173, 104

Lu, Y.-J., Loucks, R.R., Fiorentini, M., McCuaig, T.C. Evans, N.J., Yang, Z.-M., Hou, Z.-Q., Kirkland, C.L., Parra-Avila, L.A. Kobussen, A., 2016. Zircon compositions as a pathfinder for porphyry $Cu±Mo±Au$ deposits. Economic Geology Special Publication 19, 329-347.

Luo, Y., Ayers, J.C., 2009. Experimental measurements of zircon/melt trace-element partition coefficients. Geochimica et Cosmochimica Acta 73, 3656-3679.

Marshall, A., Macdonald, R., Rogers, N., Fitton, J., Tindle, A., Nejbert, K., Hinton, R., 2009. Fractionation of peralkaline silicic magmas: The greater Olkaria volcanic complex, Kenya Rift Valley. Journal of Petrology 50, 323-359.

McIntire, W. L., 1963. Trace element partition coefficients—a review of theory and applications to geology. Geochimica et Cosmochimica Acta 27, 1209-1264.

Murali, A.V., Parthasarathy, R., Mahadevan, T.M., Das, M.S., 1983. Trace element characteristics, REE patterns and partition coefficients of zircons from different geological environments—A case study on Indian zircons. Geochimica et Cosmochimica Acta 47, 2047-2052.

Olin, P.H., Wolff, J.A., 2012. Partitioning of rare earth and high field strength elements between titanite and phonolitic liquid. Lithos 128-131, 46-54.

Palin, R. M., Santosh, M., Cao, W., Li, S. S., Hernández-Uribe, D., and Parsons, A., 2020. Secular metamorphic change and the onset of plate tectonics. Earth-Science Reviews 207, 103172.

Perez-Soba, C., Villaseca, C., Del Tanago, J.G., Nasdala, L., 2007. The composition of zircon in the peraluminous Hercynian granites of the Spanish Central System Batholith. The Canadian Mineralogist 45, 509-527.

Roberts, N. M., and Spencer, C. J.,2015. The zircon archive of continent formation through time. Geological Society, London, Special Publications389, 197-225.

Rollinson, H., 1993. Using Geochemical Data: Evaluation, Presentation, Interpretation. Longman, London. 352 pp.

Rubatto, D., Hermann, J., 2007. Experimental zircon/melt and zircon/garnet trace element partitioning and implications for the geochronology of crustal rocks. Chemical Geology 241, 38-61.

Shaw, D.M., 2006. Trace elements in magmas: a theoretical treatment. Cambridge University Press, 256 pp.

Sano, Y., Terada, K., Fukuoka, T., 2002. High mass resolution ion microprobe analysis of rare earth elements in silicate glass, apatite and zircon: lack of matrix dependency. Chemical Geology184, 217-230.

Spencer, C. J., Cavosie, A. J., Raub, T. D., Rollinson, H., Jeon, H., Searle, M. P.,Miller, J.A., McDonald, B.J.,Evans, N. J., 2017. Evidence for melting mud in Earth's mantle from extreme oxygen isotope signatures in zircon. Geology45, 975-978.

Smythe, D.J., Brenan, J.M., 2015. Cerium oxidation state in silicate melts: Combined fO$_2$, temperature and compositional effects. Geochimica et Cosmochimica Acta 170, 173-187.

Smythe, D.J., Brenan, J.M., 2016. Magmatic oxygen fugacity estimated using zircon-melt partitioning of cerium. Earth and Planetary Science Letters453, 260-266.

Sun, S.-S., McDonough, W.F., 1989. Chemical and isotopic systematics of oceanic basalts: implications for mantle composition and processes. Geological Society, London, Special Publications 42, 313-345.

Szilas, K., Hoffmann, J. E., Scherstén, A., Kokfelt, T. F.,Münker, C., 2013. Archaean andesite petrogenesis: insights from the Grædefiord Supracrustal Belt, southern West Greenland. Precambrian Research236, 1-15.

Thomas, J.B., Bodnar, R.J., Shimizu, N., Sinha, A.K., 2002. Determination of zircon/melt trace element partition coefficients from SIMS analysis of melt inclusions in zircon. Geochimica et Cosmochimica Acta66, 2887-2901.

Tiepolo, M., Oberti, R., Zanetti, A., Vannucci, R., Foley, S.F., 2007. Trace-element partitioning between amphibole and silicate melt. Reviews in Mineralogy and Geochemistry67, 417-452.

Trail, D., Bruce Watson, E., Tailby, N.D., 2012. Ce and Eu anomalies in zircon as proxies for the oxidation state of magmas. Geochimica et Cosmochimica Acta 97, 70-87.

Turner, S., Wilde, S., Worner, G., Schaefer, B., Lai, Y.J., 2020. An andesitic source for Jack Hills zircon supports onset of plate tectonics in the Hadean. Nature Communications11, 1241.

Van Kranendonk, M.J., Kirkland, C.L., 2013. Orogenic climax of Earth: the 1.2–1.1 Ga Grenvillian superevent. Geology41, 735-738.

Wagner, J., Haigis, V., Künzel, D., Jahn, S., 2017. Trace element partitioning between silicate melts – A molecular dynamics approach. Geochimica et

Cosmochimica Acta205, 245-255.

Wang, X.-C., Liu, Y.-S., Liu, X.-M., 2006. Mesozoic adakites in the Lingqiu Basin of the central North China Craton: Partial melting of underplated basaltic lower crust. Geochemical Journal40, 447-461.

White, J., 2003. Trace-element partitioning between alkali feldspar and peralkalic quartz trachyte to rhyolite magma. Part II: Empirical equations for calculating trace-element partition coefficients of large-ion lithophile, high field-strength, and rare-earth elements. American Mineralogist88, 330-337.

Wu, F., Liu, X., Ji, W., Wang, J., Yang, L., 2017. Highly fractionated granites: Recognition and research. Science China Earth Sciences60, 1201-1219.

Xing, K., Shu, Q., Lentz, D. R., and Wang, F., 2020. Zircon and apatite geochemical constraints on the formation of the Huojihe porphyry Mo deposit in the Lesser Xing'an Range, NE China. American Mineralogist: Journal of Earth and Planetary Materials105, 382-396.

Yang, X. M., 2019. Using Rare Earth Elements (REE) to decipher the origin of ore fluids associated with granite intrusions. Minerals9,426.

Zhong, S., Feng, C., Seltmann, R., Li, D., Qu, H., 2018. Can magmatic zircon be distinguished from hydrothermal zircon by trace element composition? The effect of mineral inclusions on zircon trace element composition. Lithos314-315, 646-657.

Zhong, S., Seltmann, R., Qu, H., Song, Y., 2019. Characterization of the zircon Ce anomaly for estimation of oxidation state of magmas: a revised Ce/Ce* method. Mineralogy and Petrology113, 755-763.

Figure Captions

Fig. 1. Plots of reported zircon D_{REE} from natural samples and experimental studies. Note that only results published after 2000 are shown, since recent measurements are more likely to be accurate because of the higher spatial resolution of the analytical methods, therefore avoiding the effect of mineral inclusions in zircon that plagued earlier studies. The subscripts a–g indicate the references sources and are from Thomas et al. (2002), Colombini et al. (2011), Marshall et al. (2009), Sano et al. (2002), Burnham and Berry (2012), Luo and Ayers (2009), Rubatto and Hermann (2007), respectively.

Fig. 2. Three crystallization patterns modelled in this study. The melt composition changed constantly due to mineral crystallization. See Section 2.2 for more details.

Fig.3. Modelling 0 to 1% fractionation of zircon (Zrn) from a melt (pattern I). (A) CI chondrite-normalized REE patterns for remaining melts. (B) CI chondrite -normalized REE patterns for zircons in equilibrium with remaining melts. (C) Calculated zircon D_{REE} using the remaining melt composition that experienced 1% zircon fractional crystallization, with the arrow indicating the crystallization order of zircons from early to late. The inserts are full model results in increments of 0.1% crystallization. CI chondrite values are from Sun and McDonough (1989). See Section 3 for more details.

Fig.4. Modelling 0 to 1% fractionation of apatite (Ap) from a melt that experienced very limited zircon (Zrn) crystallization (pattern II). (A) CI chondrite-normalized REE patterns for remaining melts in equilibrium with apatite. The REE pattern of

thecrystallized zircon is also shown. (B) Calculated zircon D_{REE} using the remaining melt composition that experienced 1% apatite fractional crystallization. The inserts are full model results in increments of 0.1% crystallization.CI chondrite values are from Sun and McDonough (1989). See Section 3 for more details.

Fig. 5. Modelling plagioclase + zircon + apatite fractionation (pattern III). Zircon (Zrn) formed prior to apatite (Ap) but subsequent to plagioclase (Pl) and its quantity was assumed negligible. (A) CI chondrite -normalized REE patterns for remaining melt compositions in equilibrium with 0 to 40% fractionation of plagioclase. The REE patterns of zircons are also shown for comparison. (B) CI chondrite-normalized REE patterns for melts in equilibrium with fractionation of 40% plagioclase + 0–1% apatite. (C) Calculated zircon D_{REE} using the remaining melt composition that experienced fractionation of 40% plagioclase + 1% apatite. The inserts are full model results in increments of 5% crystallization for A and 0.1% crystallization for B and C. CI chondrite values are from Sun and McDonough (1989). See Section 3 for more details.

Fig.6. Plot of P vs. REE+Y of zircons from natural samples. These zircons were compiled from GEOROC database. Only 952 analyseswith full REEs and P values, as well as La contents of< 0.03 ppm were used. Zircons with La contents of ≥ 0.03 ppm werediscarded since these grains are likely contaminated by LREE-enriched mineral/melt inclusions (Zhong et al., 2019).

Fig. 7. (A–B) Modelling 0-5% pure zircon crystallization (pattern I). (C–D) Modelling 0–5% apatite crystallization after zircon (pattern II). Noticeable variations

of zircon and melt compositions, as well as significantly elevated zircon D_{REE}, are

shown. CI chondrite values are from Sun and McDonough (1989). All these scenarios

are not observed in natural granitic systems but may occur in experimental studies.

Fig.8. Comparison of melt compositions in equilibrium with >4 Ga Jack Hill zircons.

The melt REE compositions were calculated using partition coefficients from natural

samples (A) and experimental studies (B), respectively, with sources being same as in

Fig. 1. Zircon compositions are from samples 01JH36 and 01JH60 reported by

Cavosie et al. (2006). CI chondrite values are from Sun and McDonough (1989). For

the sake of comparison visually, the range of melt compositions constrained using

partition coefficients from experimental studies is also illustrated (see the shadowed

area) in A. Similar case is also in B.

Table 1 Assumed "real" partition coefficients for common REE-bearing minerals in magmatic rocks.

	Mineral/melt partition coefficients (D_R)					Melt composition (ppm)
	Apatite	Titanite	Plagioclase	Hornblende	Zircon	
Rock type	dacite	phonolite	basaltic andesite	peralkaline rhyolites	dacite	high Si adakites
References	Sano et al. (2002)	Olin and Wolff (2012)	Dunn and Sen (1994)	Marshall et al. (2009)	Sano et al. (2002)	Wang et al. (2006)
La	36	24	0.18	0.27	0.00046	44.09
Ce	48	47	0.14	0.27	0.36	79.26
Pr	64	56	0.13	0.385	0.0172	9.19
Nd	77	64	0.12	0.435	0.077	35.35
Sm	93	74	0.08	0.45	0.8	5.17
Eu	55	[a]38	0.79	0.45	1.22	1.63
Gd	127	[b]71	0.07	0.385	8	4.73
Tb	102	61	0.06	0.365	20.7	0.52
Dy	76	54	0.03	0.35	45.9	2.48
Ho	62	46	[c]0.03	0.36	80	0.43
Er	57	36	0.02	0.43	136	1.13
Tm	53	31	[c]0.02	0.57	197	0.16
Yb	48	23	0.01	0.835	277	1.03

Lu	33	20	0.01	1.3	325	0.16

Note: the superscripts indicate the measured average value (a), value estimated by the lattice strain model (b), and values interpolated from neighboring D (c). The high Si adakite composition was used as the starting melt of the modelling calculation.

Graphical abstract

Highlights

- Zircon D_{REE} will vary if REE-enriched minerals crystallize subsequent to zircon.

- Natural samples give more reliable zircon D_{REE} than experimental studies.

- The old Jack Hill zircons may be derived from LREE enriched melts.
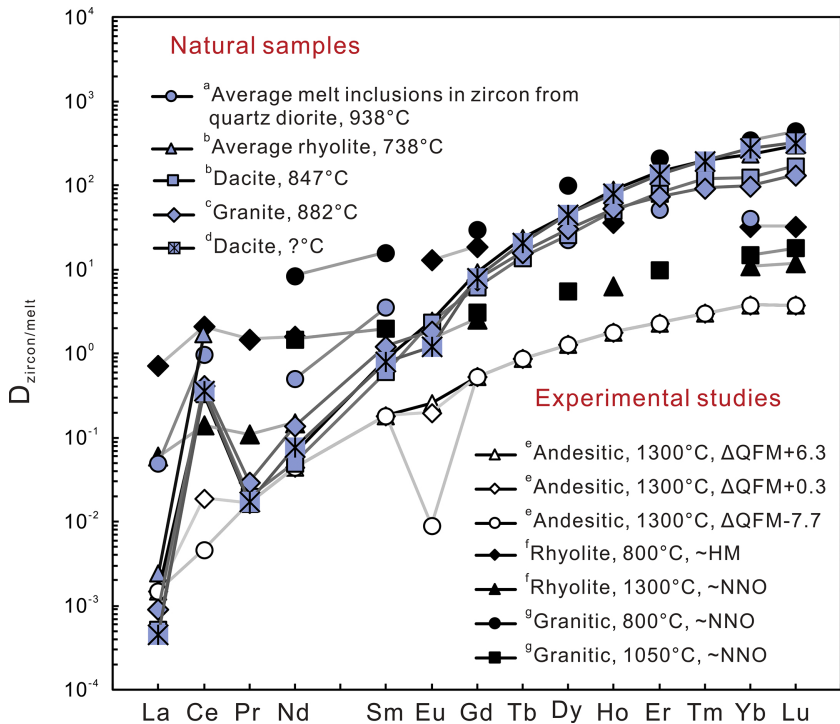
Figure 1
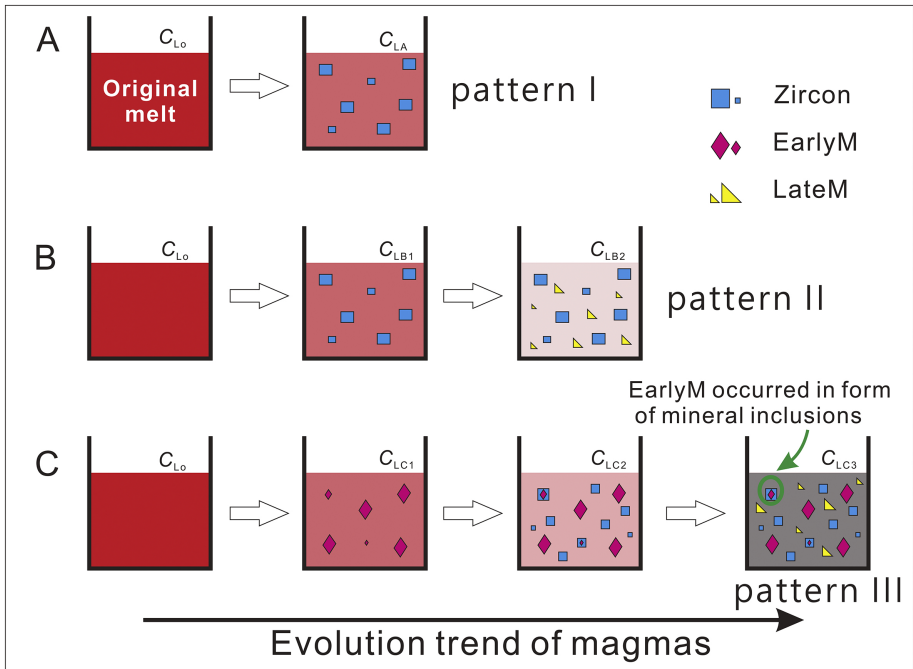
Figure 2
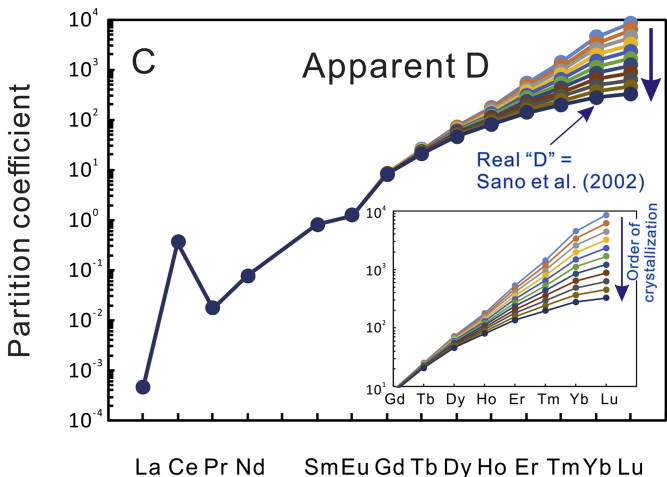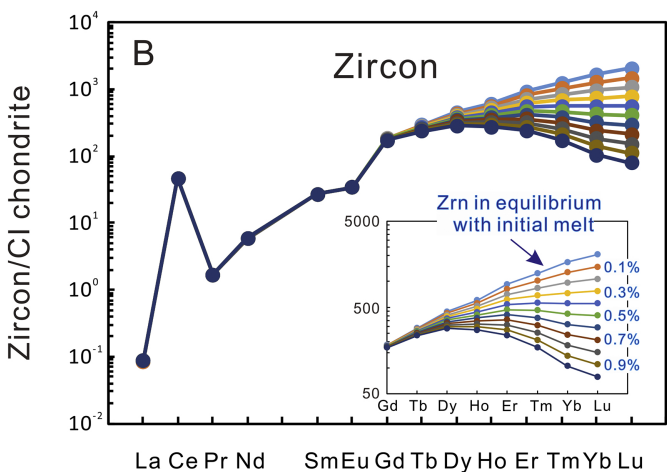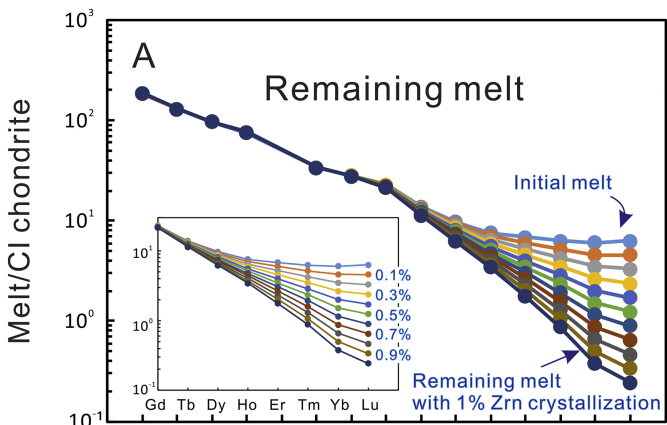
Figure 3
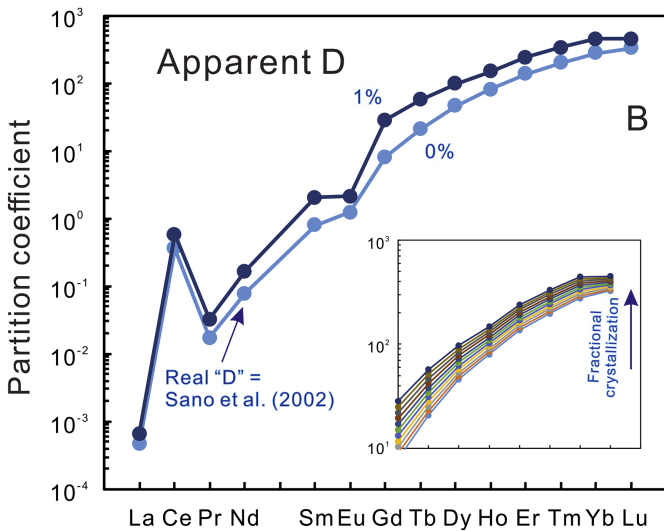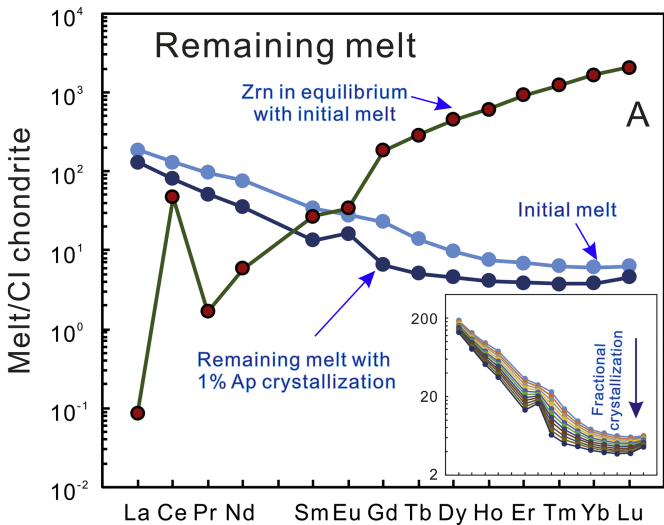
Figure 4
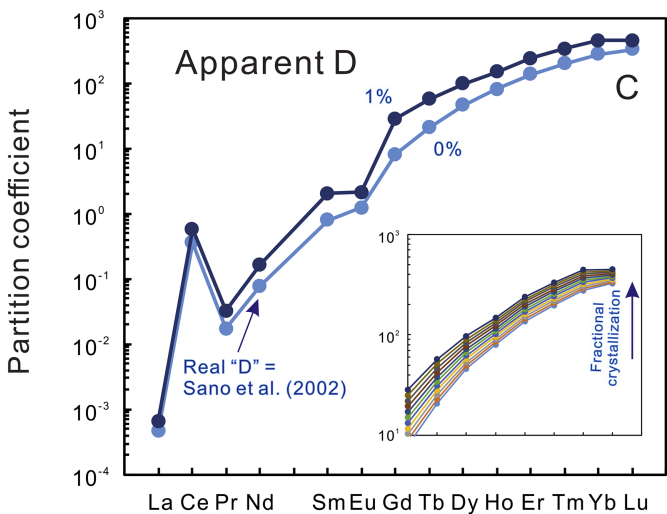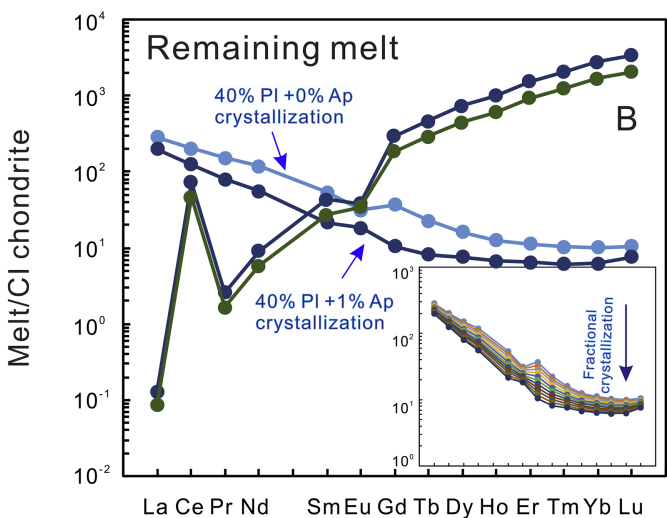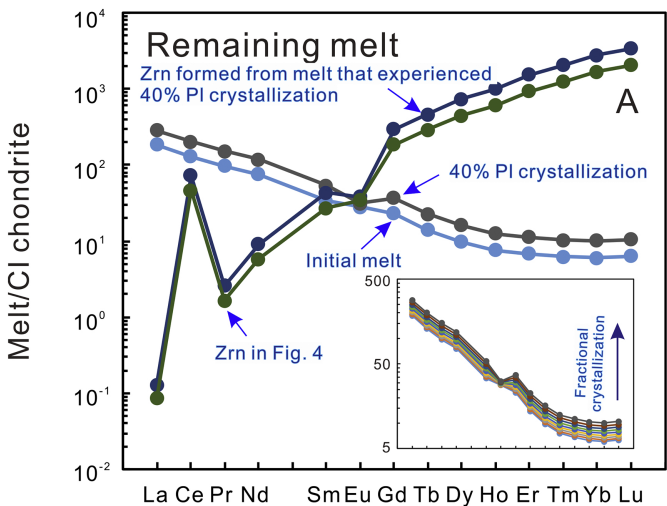
Figure 5
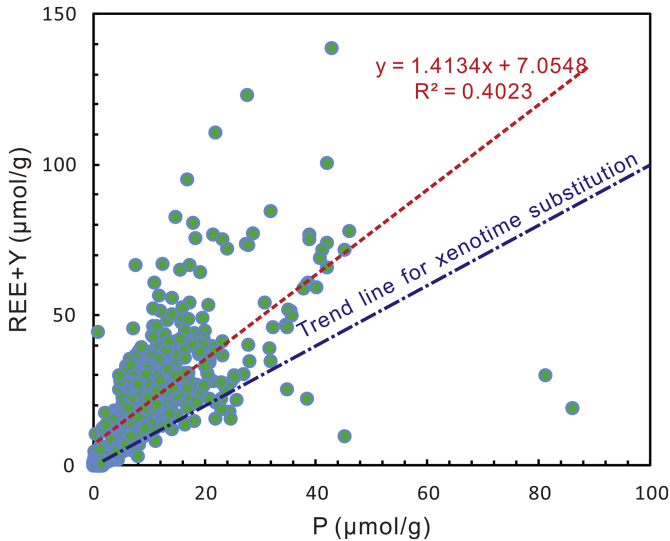
Figure 6

Figure 7

Figure 8